

Anthropogenic aerosol effects on convective cloud microphysical properties in southern Sweden

By E. FREUD^{1*}, J. STRÖM¹, D. ROSENFELD², P. TUNVED¹ and E. SWIETLICKI³,

¹Department of Applied Environmental Science, Stockholm University, Sweden; ²Department of Atmospheric Sciences, Hebrew University of Jerusalem, Israel; ³Division of Nuclear Physics, Department of Physics, Lund University, Sweden

(Manuscript received 21 November 2006; in final form 12 November 2007)

ABSTRACT

In this study, we look for anthropogenic aerosol effects in southern Scandinavia's clouds under the influence of moderate levels of pollution and relatively weak dynamic forcing. This was done by comparing surface aerosol measurements with convective cloud microphysical profiles produced from satellite image analyses.

The results show that the clouds associated with the anthropogenic-affected air with high PM_{0.5}, had to acquire a vertical development of ~3.5 km before forming precipitation-sized particles, compared to less than 1 km for the clouds associated with low PM_{0.5} air-masses.

Additionally, a comparison of profiles with precipitation was done with regard to different potentially important parameters. For precipitating clouds the variability of the cloud thickness needed to produce the precipitation (Δh_{14}) is directly related to PM_{0.5} concentrations, even without considering atmospheric stability, the specific aerosol size distribution or the aerosols' chemical composition. Each additional 1 $\mu\text{g m}^{-3}$ of PM_{0.5} was found to increase Δh_{14} by ~200–250 m.

Our conclusion is that it is indeed possible to detect the effects of anthropogenic aerosol on the convective clouds in southern Scandinavia despite modest aerosol masses. It also emphasizes the importance of including aerosol processes in climate-radiation models and in numerical weather prediction models.

1. Introduction and background

It has been known for some time (Twomey, 1974) that anthropogenic aerosols have the potential to affect cloud microphysics by serving as additional cloud condensation nuclei (CCN), thus causing the polluted clouds to consist of more and smaller droplets for a given amount of cloud water, compared to clouds unaffected by pollution. The redistribution of cloud water near the bases of polluted clouds, might in turn, affect the duration and occurrence of other microphysical processes within the cloud (such as coalescence, rainout, etc.), which may cause further changes in precipitation characteristics, latent heat release, vertical circulation, etc. Thus, a small initial perturbation might be transferred to much larger scales (Nober et al., 2003). The inadequate knowledge about these processes and the resulting large uncertainty are important reasons for climate models being difficult to reconcile with observations (Kaufman and Fraser, 1997).

The anthropogenic aerosol effects on clouds have already been documented using remote sensing methods (e.g. Kaufman

and Fraser, 1997; Rosenfeld, 2000), in situ measurements (e.g. Hudson and Yum, 2001; Heymsfield and McFarquhar, 2001; Yum and Hudson, 2002; Andreae et al., 2004) and cloud models (e.g. Khain et al., 2004). Previous studies regarding aerosol perturbations of convective clouds have focused on regions where the perturbation in aerosol properties has been very large and the dynamic forcing very strong. For example, biomass burning in South America (Freud et al., 2005) and Indonesia (Rosenfeld, 1999) and dust episodes in the Mediterranean and the Atlantic Ocean (Rosenfeld et al., 2001). We are not aware of such studies performed for cases at higher latitudes where the dynamic and thermodynamic forcing is usually smaller and without extreme conditions, such as forest fires or large industrial pollution sources, resulting in aerosol masses larger by an order of magnitude compared to the aerosol mass on the most polluted day in this study (Freud et al., 2005 and Table 1). We ask the question: is it possible to detect an anthropogenic aerosol effect on convective clouds even for relatively small perturbations in aerosol properties? The area of investigation is Scandinavia or more precisely the southern half of Sweden.

The Scandinavian Peninsula, which Sweden is a part of, is surrounded by the North and Norwegian Seas to the west and the Arctic sea to the north. The Baltic Sea and the Gulf of Bothnia enclose the peninsula at the south and east and separate it from

*Corresponding author.
e-mail: eyal.freud@mail.huji.ac.il
DOI: 10.1111/j.1600-0889.2007.00337.x

Table 1 Summary of the related information and parameters of all profiles

No.	Date and time ^a	Satellite	Lat ^b	Lon ^b	PM _{0.5} ^c	PM _{2.5}	PM ₁₀	Station ^d	Base T ^e	Top T ^f	dT ^g	CAPE ^h	L ⁱ	Azimuth ^j	Distance ^k	ΔT ₁₄ ^l
1	07-Apr-04 11:40	Aqua	56	13	-	9.00	9.70	-	-6	-33	27	905	0	223.7	7.2	10.0
2	17-Apr-04 10:30	Terra	58	13	15.77	26	29.3	V	-3	-20	17	0	5	142.8	8.6	-
3	09-May-04 11:40	Aqua	57	15	11.32	25.8	32.4	A	2	-38	40	0	-1.5	88.7	15.6	24.6
4	09-May-04 11:40	Aqua	59	16	11.32	25.8	32.4	A	-9	-26	17	1135	-1.5	88.7	15.6	18.5
5	20-May-04 11:20	Aqua	59	17	0.4	2.9	3.4	A	-14	-21	7	0	4	315.4	13.6	-
6	21-May-04 12:05	Aqua	57	15	0.9	2.4	2.8	V	-8	-20	12	0	5	296.3	23.6	-
7	22-May-04 11:10	Aqua	60	16	0.88	1.8	5	A	-8	-42	34	884	-1	298.5	15.4	7.1
8	24-Jun-04 11:50	Aqua	59	16	11.2	13.3	16.3	A	9	-48	57	0	1	249.7	19.5	21.0
9	25-Jun-04 10:45	Terra	60	17	6.3	9	17.6	A	-1	-44	43	710	0.5	260.1	17	12.4
10	01-Jul-04 10:10	Terra	61	17	7.22	9.2	18.3	A	4	-15	19	0	1	255.5	17.6	-
11	27-Jul-04 10:45	Terra	57	15	4.2	6.2	6.6	V	0	-35	35	0	-2	295.7	8.4	13.3
12	04-Aug-04 11:45	Aqua	60	17	13.7	-	23	A	12	-50	62	240	-1	105.8	16.2	24.2
13	05-Aug-04 10:40	Terra	60	15	14.4	-	31.8	A	7	-16	23	0	-0.5	109.4	13.9	16.8
14	05-Aug-04 10:40	Terra	60	18	14.4	-	31.8	A	2	-5	7	0	0.5	109.4	13.9	-
15	06-Aug-04 11:35	Aqua	60	14	12.5	18.5	17.8	A	8	-41	49	2197	-3	113.6	10.5	19.7
16	10-Aug-04 11:10	Aqua	57	18	4.2	5	8	V	13	0	13	0	3	20	5.5	-
17	21-Aug-04 10:40	Terra	61	16	4.7	9	-	A	4	-13	17	330	-2	283.4	11.5	6.0
18	22-Aug-04 11:35	Aqua	60	17	1.52	6.3	-	A	-2	-46	44	976	-3.5	311.2	10.6	2.9
19	22-Aug-04 11:35	Aqua	57	15	0.72	-	-	V	-1	-37	36	0	-2	315.7	15.1	4.4
20	22-Aug-04 11:35	Aqua	58	13	1.52	6.3	-	A	-3	-13	10	276	-3	315.7	15.1	1.0
21	28-Aug-04 10:45	Terra	58	13	2.8	5	11.7	A	3	-15	18	0	1	271.2	25.4	6.4

^aDate and time (UTC) of satellite pass.

^bApproximate latitude and longitude of the centre of the cloud domain in degrees north and east, respectively.

^cAerosol mass of particles with diameter <0.5 μm [μg m⁻³].

^dGround station closer to cloud domain for which PM0.5 is shown. 'A' for Aspreten; 'V' for Vavihill.

^eWarmest temperature of cloudy pixel [°C].

^fColdest temperature of cloudy pixel [°C].

^gTemperature difference between coldest and warmest cloudy [°C], represents cloud thickness

^hConvective available potential energy [J kg⁻¹].

ⁱ(four-layer best) Lifted Index, a measure of atmospheric instability.

^jThe azimuth of the centre of gravity point of the 72 h back trajectory, in relation to the aerosol measurement station (Aspreten or Vavihill) and the north [°].

^kThe distance of the centre of gravity point of the 72 h back trajectory to the aerosol measurement station (Aspreten or Vavihill) [°].

^lThe difference between cloud base temperature and the temperature at which the cloud top particle effective radius crosses 14 μm [°C].

continental Europe. Sweden is located in the high mid-latitudes and therefore is affected periodically by different air-masses with very dissimilar aerosol properties (Tunved et al., 2005). Typically, air-masses arriving from the north or west are expected to be relatively clean and to contain small numbers of accumulation mode particles (~ 100 – 1000 nm in diameter), while air passing over continental Europe is expected to contain more accumulation mode particles as a result of the larger anthropogenic sources of aerosols and precursor gases over continental Europe (Tunved et al., 2003). The sizes of the accumulation mode particles and their affinity for water enable them to serve as CCN active at lower supersaturations than required for smaller particles. The local contribution of anthropogenic aerosols in Scandinavia is relatively small due to the fairly low population density, especially during summer months when less wood is burned for domestic heating, which can be a major source of CCN (Hudson et al., 1991).

In this study, we will make use of ground based aerosol size distributions and derived cloud microphysical properties from satellite imagery. The instrumentation and tools used to collect the aerosol and cloud data will be briefly described in Section 2. Section 3 will present and discuss a comparison of cloud microphysical properties for characteristic air-masses with a high and a low aerosol loading. All 21 cases analysed in this study are then compared, and the derived cloud microphysical profiles are discussed with respect to observed aerosol properties and the dynamic stability of the air. Section 4 will summarize this study and present its conclusions.

2. Methods and instrumentation

In order to be able to answer our research question, regarding the ability to detect any anthropogenic aerosol effect on the convective clouds in Scandinavia, we have to be able to characterize the aerosols within a certain air-mass and determine their origin. The latter can be easily achieved by using an online back-trajectory model, such as HYSPLIT (<http://www.arl.noaa.gov/ready/hysplit4.html>). But the specific aerosol characteristics (size and composition) at a certain place and time are strongly affected by the processes of aerosol dynamics that took place during the history of the air-mass. These processes include aerosol deposition (wet and dry), nucleation of new particles, coagulation, processes within the clouds and more.

2.1. Aerosol measurements

In this study, our main aerosol measurements are size distributions from two rural (background) stations (see locations in Fig. 3c). The first station is located at Aspvreten (58.8°N , 17.4°E , 25 m. a.s.l.), about 70 km southwest of Stockholm, in an area scarcely populated and approximately 2 km from the Baltic Sea coast. The size-range of the measured aerosols is between ~ 9 and ~ 500 nm in diameter. The second station is located at

Vavihill (56.01°N , 13.09°E , 172 m. a.s.l.), about 20 km east of Helsingborg and some 60 km NNE of Copenhagen and Malmö. Aerosol sizes measured there are between ~ 3 and ~ 900 nm, but in order to be able to compare the aerosol masses between the two stations, we have truncated the size distribution measured at Vavihill at 500 nm, the largest detectable aerosol diameter in the Aspvreten data. Both stations use Differential Mobility Particle Sizers (DMPS) for measuring the aerosol size distributions.

The DMPS consists of two main components. One is the Differential Mobility Analyser (DMA), which after acquiring a known charge distribution as a function of particle size using a radioactive neutralizer, separates a certain sized particle from the rest of the particles due to their different electrical mobility. The selected particles (within a narrow size range) are counted optically using a condensation particle counter (CPC). By changing the electric field (voltage), particles in different size-ranges can be selected and counted. A full scan over all sizes is performed in 5–10 min. The information is then inverted to a particle number size distribution.

To simplify the comparison, the particle mass concentration was calculated using the size distributions. The aerosols were assumed to be spherical and have a density of 1.5 g cm^{-3} . In view of the fact that the mass (or volume) is proportional to the cube of the particle diameter, the integrated aerosol mass over particles smaller than 500 nm (henceforth, $\text{PM}_{0.5}$) will be very sensitive to small changes in the number density of accumulation mode particles.

The air which arrives from between the north and the west is expected to have a low $\text{PM}_{0.5}$ because it is less prone to anthropogenic aerosol and precursor gas emissions that would result in a relatively large number of accumulation mode particles. However, although devoid of anthropogenic sources, the forested regions over boreal Scandinavia do contribute to both number and mass increase of aerosols. Terpenes are probably key-candidates in this process, serving as precursors of low and semi-volatile compounds capable of partitioning in the particle phase. Occasions of rapidly increasing number density of nanometer sized particles and subsequent growth are especially frequent in the spring and the autumn (Kavouras et al., 1998; O'Dowd et al., 2002; Kulmala et al., 2004; Tunved et al., 2006). The so called 'nucleation events' contribute significantly to the aerosol number, but little to the aerosol mass (in absolute terms, i.e. less than $\sim 1 \mu\text{g m}^{-3}$) compared to anthropogenic activities.

Air-masses that pass over continental Europe, on the other hand, are expected to have a relatively high $\text{PM}_{0.5}$ due to the anthropogenic emissions of accumulation mode particles and the growth of smaller aerosols into this size range because of in-cloud processes and coagulation. These accumulation mode particles make up nearly the entire aerosol mass and cause it to be significantly larger than would be the case without anthropogenic sources.

Measurements of $\text{PM}_{2.5}$ and PM_{10} (mass of particulate matter with aerodynamic diameter smaller than 2.5 and 10 μm ,

respectively) were also made at both stations using Tapered Element Oscillating Microbalance (TEOM) instruments (Patashnick and Rupprecht, 1991; Parikh, 2000). A filter dynamics measurement system (FDMS), which allows to measure the volatile aerosols without the need to correct the TEOM measurements for them (Schwab et al., 2006), was used only for the $PM_{2.5}$ measurements at Aspvreten. In contrast to the calculated $PM_{0.5}$, $PM_{2.5}$ and PM_{10} are standard measurements, which are measured directly. These measurements are sensitive to the few supermicron particles, but less to the Aitken (~ 30 – 100 nm) and accumulation mode particles which comprise the most of the CCN population, and therefore are expected to be less related than $PM_{0.5}$ to the cloud properties.

2.2. Cloud microphysical analysis

Clouds consist of small water droplets and ice particles, and are formed as a result of cooling the air to the temperature at which it reaches its saturation pressure for water vapour (over liquid water or ice). Additional cooling will cause supersaturation and condensation of the excess water vapour onto the pre-existing larger and more hydrophilic particles that activate as CCN. The number of activated CCN depends on aerosol size and composition and the cloud supersaturation, which is mainly determined by the updraft speed at cloud base.

In deep convective clouds, various microphysical processes, or phases, may exist. These processes generally lead to the growth of the cloud particles, and eventually to the formation of precipitation-sized particles that can fall through the updraft. These microphysical phases, from cloud base to cloud top, are called: *diffusion (condensational growth)*, *coalescence*, *rainout (warm rain)*, *mixed phase* and *glaciation* (Rosenfeld and Lensky, 1998). They mainly depend on the temperature, the size distribution of the cloud particles, the updrafts, the ambient air and the nature of the aerosols. There are of course interactions between these factors, so one should be cautious while trying to estimate the effects of the different factors on cloud microphysical processes.

In situ airborne measurements outside and within the clouds may be the most straightforward method to study the effect of the aerosol on cloud microphysics, but this method requires actual cloud flights. Here, we apply remote sensing methods to study the microphysical processes in the Scandinavian convective clouds. Convective clouds were chosen for the analysis because they are directly fed by the boundary layer aerosols and because the satellite can only see the tops of the clouds. Hence, one can take advantage of the fact that convective clouds have tops at various heights and this effectively produces a vertical microphysical profile. By implementing this method, one has to assume that cloud tops at different heights represent (microphysically) a well-developed cloud. This assumption was found to be valid by using both remote sensing (Lensky and Rosenfeld, 2005) and in situ aircraft measurements (Freud et al., 2005).

In order to produce vertical profiles of the cloud microphysical phases for various aerosol loads, multispectral data were collected using MODIS sensors onboard AQUA and TERRA orbital satellites. This information was used to calculate the cloud top effective radius (henceforth, r_e) of the cloud particles, which is a commonly and widely used measure that relates to the size distribution of the particles in the cloud. The effective radius is proportional to the ratio between the total volume and surface area of the cloud droplets and is therefore related to the absorption and scattering of the solar radiation by the cloud droplets, respectively. This relationship enables the calculation of r_e for each cloudy pixel. Combining this information with the thermal radiation, allows the construction of a vertical profile of r_e as a function of the temperature, from which the microphysical phases of the cloud can be identified. The methods used for the construction of the temperature- r_e relationship and the identification of the microphysical phases from satellite images, are thoroughly described in Rosenfeld and Lensky (1998).

In this study, we implemented the methods of Rosenfeld and Lensky (1998), but had to find first suitable satellite images for this analysis. The selection of scenes used in the analysis is done manually and thus is very labour intensive. This is why the data set was limited to the period between April and September, 2004. During the other months of the year deep convection over Scandinavia is very rare and water-clouds are more difficult to find. Initially, days which presented relatively low or high derived aerosol masses were selected in order to examine if suitable convection occurred. Suitable here means that convective clouds with tops at various heights were present over the southern half of Sweden and there were no obscuring high clouds or anvils. Images that were found suitable for further processing were colour-coded in a way that allowed the cloud microphysical properties to be distinguished by producing a composite Red–Green–Blue (RGB) image (see example in Fig. 5). The guiding principle in choosing a cloud field, on which to calculate the cloud top particle effective radius versus the cloud top temperature (henceforth, T – r_e) profile, was to include clouds at various stages in their evolution. Thus capturing a range of cloud top temperatures. In addition, the clouds had to be within a relatively homogeneous area, i.e. where we had no obvious reason to suspect that there were large differences in the aerosol properties within the selected region. These situations could for instance be front or squall line passages. Regions indicating ice phase and anvil clouds were intentionally avoided.

The selection procedure resulted in 19 scenes from 17 different days. From these images 21 independent profiles of r_e were plotted against the cloud top temperatures. By ‘independent’ we mean that the profiles were derived for different days or regions far from each other and with different thermodynamic conditions and/or aerosol properties.

Different updraft speeds at cloud base, mainly determined by the thermodynamic instability of the atmosphere, may result in different cloud microphysical properties given otherwise same

initial conditions. In case of a very unstable atmosphere, strong updrafts can lead to high supersaturation near the cloud-base and the nucleation of many smaller aerosols (Rosenfeld et al., 2002), this may cause the analysed profile to appear more polluted than the aerosol properties alone may indicate. Therefore, it is important to take the atmospheric instability into account when trying to evaluate the aerosol effect on the clouds. For each profile we calculated Convective Available Potential Energy (CAPE) and (four-layer best) Lifted Index (the minimum value of the subtraction act of the temperature that a parcel would have if it were adiabatically elevated from each of the four lowermost model levels to the 500 mb level, from the temperature of the environment at that level) from the available meteorological data and the nearest available sounding in time and space.

3. Results and discussion

Table 1 displays some of the main parameters derived from each profile or related to it. The $PM_{0.5}$ shown for each profile is calculated from the aerosol size distribution at the ground station (Aspvreten or Vavihill) closest to the cloud domain or that is a priori expected to be the most representative. In general, there is good agreement in $PM_{0.5}$ between the two stations ($R = 0.89$, not shown), indicating that despite the ~ 500 km distance between the stations, the $PM_{0.5}$ is representative of quite a large area and is affected primarily by the origin of the air-masses that cover the southern half of Sweden. Examining the (HYSPLIT) calculated back-trajectories for all our analysed days, showed a strong relationship between the direction from which the air-mass arrived and $PM_{0.5}$ ($R = -0.89$, see Table 2). Figure 1a displays $PM_{0.5}$ measured at Vavihill and Aspvreten, as the distance from the centre of the graph, versus the azimuth of the centre of gravity of the 72-h back-trajectory, from which the air-mass has arrived. It can be clearly seen that air-masses arriving from between the north and the west, that is, air-masses that have travelled a long way above the North Atlantic, are associated with small $PM_{0.5}$

(typically smaller than $2 \mu\text{g m}^{-3}$). On the other hand, air-masses arriving from an azimuth with southerly component and especially easterly component (continental Europe) are associated with the higher $PM_{0.5}$ (typically greater than $5 \mu\text{g m}^{-3}$).

We have repeated the same exercise as shown in Fig. 1a, but instead of plotting the aerosol mass in the radial axis, we plotted (four-layer best) Lifted Index, cloud vertical extent, cloud base temperature and cloud top temperature (Fig. 1b–e, respectively). None of these parameters show a directional dependence with respect to the origin of the air-mass as strong as the $PM_{0.5}$ (maybe except for cloud base temperature which shows a small directional dependence). This also implies that the correlation between the aerosol mass and the above-mentioned parameters is not very high and therefore helps us to separate the effect of the aerosol mass on the cloud microphysical properties from the other factors.

3.1. Comparison of two cases

As a first stage, we were interested in finding two cases that are as similar as possible in all parameters that have the potential to affect the r_c vertical profile, except for the aerosol properties. This enables us to eliminate other possible explanations as the causes for the different shapes of the profiles. The profile that was chosen to represent a low aerosol mass day was from August 22, 2004 (profile #19 in Table 1), and a profile from May 9, 2004 (#3 in Table 1) was chosen to represent the high aerosol mass day (although there were a couple of days with slightly greater aerosol masses but their other properties were less comparable with the low aerosol mass case). In both cases the lower atmosphere was only slightly unstable, as indicated by the (four-layer best) Lifted Index of about $-2 \text{ }^\circ\text{C}$ (source: http://www.cdc.noaa.gov/cgi-bin/db_search/SearchMenus.pl). Based on the temperature profiles for the 2 days, presented in Fig. 2, no CAPE could be derived. Thus, the absence of CAPE and the low values of (four-layer best) Lifted Index suggests that neither day was characterized by

Table 2. Correlation table between all parameters shown in Table 1 (for variable explanation, check the footnotes of Table 1). Correlations that are significant at the 0.01 and 0.05 levels are marked by * and **, respectively

	PM 0.5	PM 2.5	PM 10	Base T	Top T	dT	CAPE	LI	Azimuth	Distance	ΔT_{14}
PM0.5	1.00*										
PM2.5	0.92*	1.00*									
PM10	0.89*	0.95*	1.00*								
Base T	0.51**	0.22	0.35	1.00*							
Top T	-0.05	-0.18	0.04	0.02	1.00*						
dT	0.25	0.27	0.12	0.40	-0.91*	1.00*					
CAPE	0.08	0.22	0.01	-0.04	-0.42	0.37	1.00*				
LI	0.03	-0.10	-0.29	-0.22	0.40	-0.46	-0.48	1.00*			
Azimuth	-0.89*	-0.92*	-0.88*	-0.26	0.15	-0.25	-0.23	0.14	1.00*		
Distance	-0.16	-0.15	-0.04	-0.08	-0.07	0.03	-0.25	0.16	-0.02	1.00*	
ΔT_{14}	0.91*	0.81*	0.70**	0.61**	-0.41	0.59**	0.05	0.27	-0.84*	0.08	1.00*

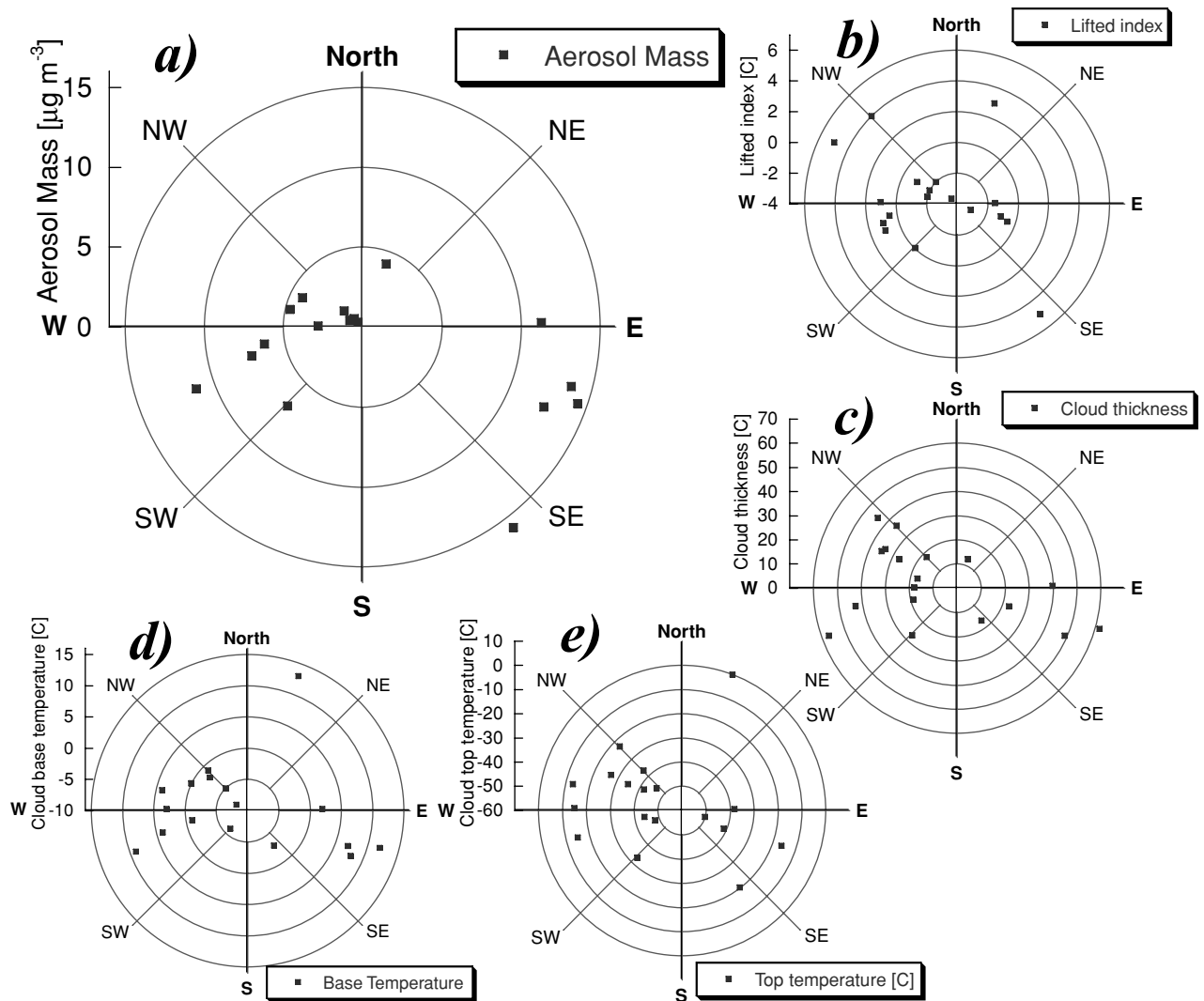


Fig. 1. (a) The relation between aerosol mass ($PM_{0.5}$) in southern Sweden (Vavihill and Aspveten) and the relative azimuth from which the air-mass arrived for all analysed days. This was derived from the location of the centre of gravity of the air-mass's 72 h back-trajectory (using HYSPLIT back-trajectory model). The distance from the centre corresponds to the aerosol mass. (b)–(e) Same as (a) but for (four-layer best) Lifted Index, cloud thickness, cloud base temperature and cloud top temperature, respectively.

strong updrafts. Moreover, the cloud-base temperatures as well as the vertical extent of the clouds were similar, and the analysed cloud fields covered approximately the same geographical area marked as green quadrangles in Fig. 5. The synoptic conditions and the back-trajectories can be seen in Fig. 3. Both days are associated with a low-pressure system and cyclonic flows, but the different locations of the depressions' centre cause the different flows and different air-masses. Panels c and d in Fig. 3 show that on August 22 the air-mass arrived from the North Atlantic while on May 9 the air-mass came from western Russia and the Baltic states and therefore was expected to contain more anthropogenic aerosols. The size distributions for the two cases, shown in Fig. 4, are very different. On May 9 (high aerosol loading), the total number density ($D_p > 9 \text{ nm}$) of 3200 cm^{-3} is controlled by par-

ticles larger than approximately 50 nm in diameter, yielding an integrated $PM_{0.5}$ of $11.3 \mu\text{g m}^{-3}$. The open size distribution towards larger particles indicates that this value is underestimating the total aerosol mass, which can be more than five times larger as can be seen by the value of PM_{10} in Table 1. On August 22 (low aerosol loading), the total aerosol number density (12000 cm^{-3}) is controlled by particles smaller than approximately 40 nm in diameter yielding an integrated aerosol mass of only $0.7 \mu\text{g m}^{-3}$.

Figure 5 shows a composite RGB image for the two selected cases, based on the satellite data in three channels. The red colour corresponds to the relative reflectance of visible wavelength (centred at $\sim 0.5 \mu\text{m}$). The green is near infrared (NIR) reflectance centred at $3.7 \mu\text{m}$ and is strongly related to r_e . The

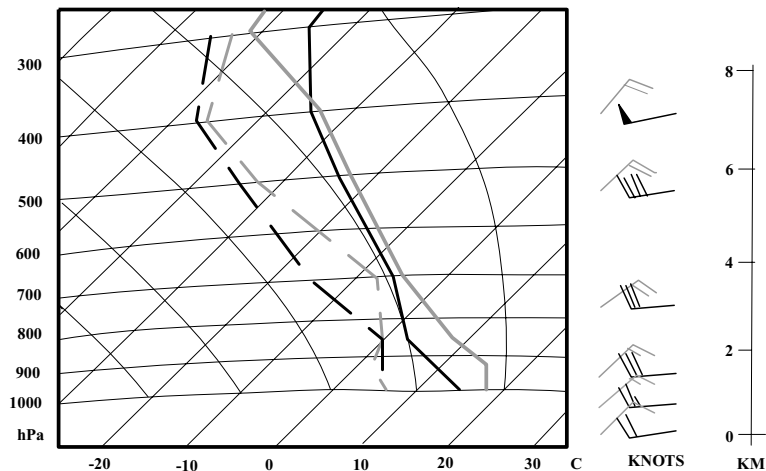


Fig. 2. Comparison of the sounding data (at 57°N, 15°E) of the two selected cases on a thermodynamic chart. The grey curve is for May 9, 2004 and the black is for August 22, 2004. The solid lines represent the temperature profiles and the broken lines represent the Dew point profiles. The wind vectors at different heights are shown to the right. There is no positive CAPE for both cases and the (four-layer best) Lifted Index indicates only slightly unstable lower atmosphere. Lines not labelled in the graph are pseudo-adiabats. (Source: <http://www.arl.noaa.gov/ready/amet.html>).

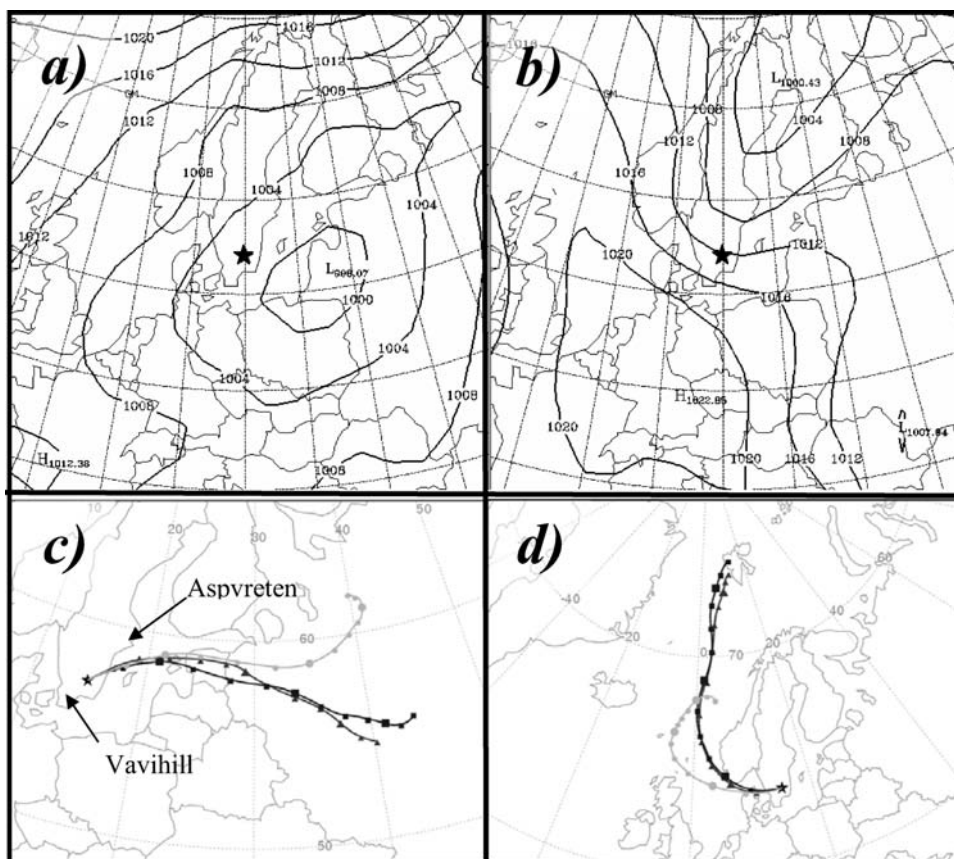


Fig. 3. (a) and (b) Sea level pressure for May 9, 2004 (left-hand side) and August 22, 2004 (right-hand side). (c) and (d) HYSPLIT modelled 72 h back-trajectories in three levels (triangles: 500, squares: 1500 and circles: 5000 m a.s.l) for the same days, respectively. The black stars in all panels represent the centre of the cloud domain. The black arrows in panel (c) point to the location of the aerosol measurement stations of Aspvreten and Vavihill. Note the different location of the centres of the depressions (panels a and b) causing different wind directions.

blue corresponds to the thermal channel of 10.8 μm , so warmer is bluer. Rosenfeld and Lensky (1998) discuss thoroughly the meaning of each composite colour, but it is enough to see here that the pollution affected clouds (Fig. 5a) are less red and more

orange than the clouds not affected by pollution (Fig. 5b) as a result of larger reflectance in NIR (more green in this ‘RGB’ image) caused by smaller droplets. This qualitative view can become quantitative by plotting the $T-r_c$ profile, thus observing

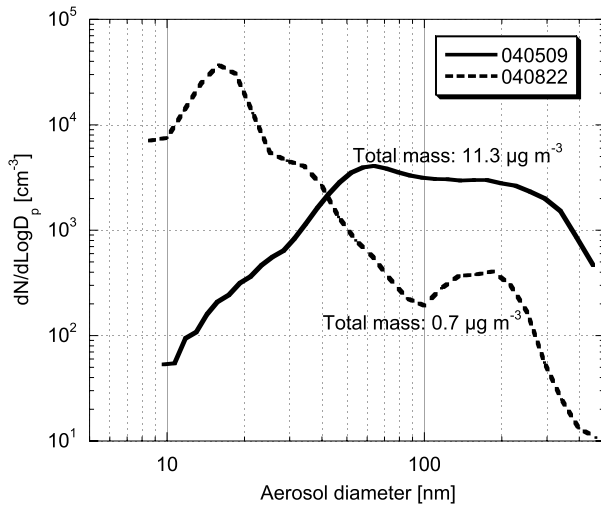


Fig. 4. The aerosol number size distributions for May 9, 2004 (solid curve – from Aspvreten) and August 22, 2004 (dashed curves – from Vavihill) and their PM_{0.5}.

variations in r_e with height. Figure 6 does so by displaying the 30th percentile from the bottom of the r_e distribution for the same cloud top temperature, in one degree (°C) increments. The 30th percentile is chosen in order to examine the younger developing clouds, before the ice processes become significant, because the ice absorbs at 3.7 μm more than water and this induces falsely large r_e and also because ice is less dense and therefore an ice particle is larger than a droplet with the same mass. Anyway, choosing the median, or even the 70th percentile of r_e , did not weaken the relationships discussed below. It is obvious that on the high aerosol loading day, the growth of r_e is inhibited by the slow condensational growth, up to the temperature of $\sim(-)18^\circ\text{C}$, where apparently ice particles form in the cloud and

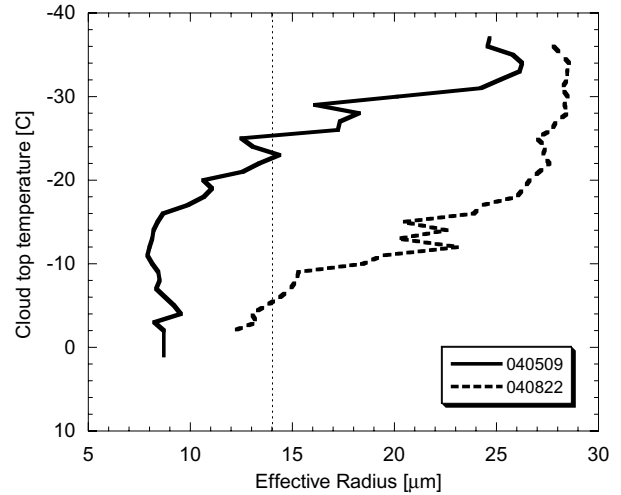


Fig. 6. Vertical profiles of the cloud top particle effective radii (30th percentile, three-point running average for reducing the ‘noise’) versus the cloud top temperature for May 9, 2004 (the ‘dirty’ case – solid curve) and August 22, 2004 (the ‘clean’ case – dashed curve). The profiles were derived from the domains marked by the green quadrangles in Fig. 5. The dashed vertical line at $r_e = 14 \mu\text{m}$ marks the precipitation threshold (Rosenfeld and Guttman, 1994).

cause a rapid increase r_e . On the other hand, on the low aerosol loading day, r_e grows much faster with height, indicating strong coalescence processes from close to the cloud base. r_e crosses the 14 μm precipitation threshold (Rosenfeld and Guttman, 1994) at a relatively shallow cloud depth. This means that the clouds associated with low aerosol loading do not need to have a large vertical extent in order to start precipitating from their tops. Full *glaciation* of the cloud seems to appear already at temperatures as warm as $\sim(-)17^\circ\text{C}$, indicating efficient precipitation processes.

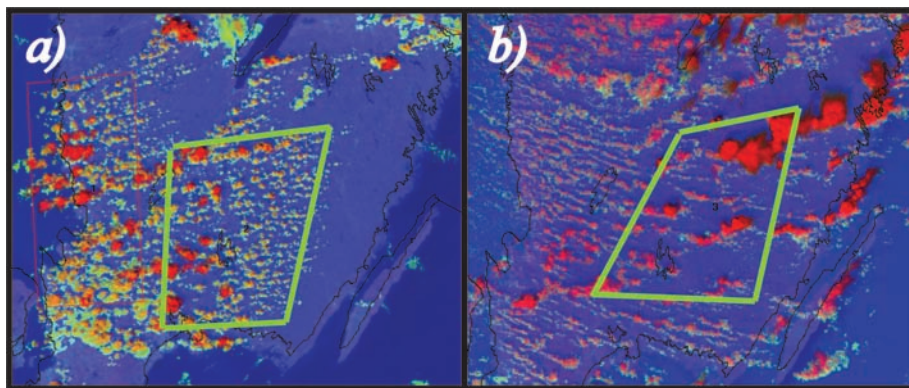


Fig. 5. Aqua/Modis images for (a) May 9, 2004, 11:40 UTC and (b) August 22, 2004, 11:35 UTC. The colour is composed of red for visible reflectance, green for 3.7 μm reflectance and blue for the 10.8 μm brightness temperature. The green quadrangles denote the domains for which the cloud microphysical profiles were calculated. Note that clouds with smaller r_e appear to be greener. For a complete colour palette and implications see Rosenfeld and Lensky (1998).

3.2. All profiles

As mentioned in the previous section, the two cases with the most similar properties, except for aerosol mass, were chosen to represent the low and high aerosol loading cases. The other scenes from other days and locations in Sweden had a range of depths, cloud base temperatures, stability indices and, of course, aerosol masses (see summary in Table 1).

In order to visually compare cases, cloud base temperatures were normalized. In Fig. 7 the cloud top particle effective radii of all 21 cases are plotted as a function of degrees below the cloud base temperature. In Fig. 7a–d, the different profiles are grey shaded according to (a) aerosol mass observed at the nearest ground based station ($PM_{0.5}$); (b) (four-layer best) Lifted Index as a measure of instability; (c) cloud base temperature and (d) cloud thickness (which is also strongly related to cloud top temperature—see Table 2). It is clear that the variable that gives the most systematic structuring in tint is $PM_{0.5}$ (panel a), especially r_e of up to $\sim 25 \mu\text{m}$. At larger r_e and far from the clouds' bases, the coalescence and ice processes may be well developed and cause the rapid increase in r_e . The cloud base temperature (Fig. 7c) seems to give some structure in the tints, but it is difficult to see anything from the (four-layer best) Lifted Index and the cloud thickness (Fig. 7b and d, respectively). The apparent relation between the aerosol mass and the shape of the $T-r_e$

profiles suggests that the $PM_{0.5}$ can account for a large part of the variation in the microphysical profiles. But this does not mean that aerosol mass itself is the direct cause for the microphysical variations, this is most certainly due to its strong dependence on the number of larger aerosols (typically larger than 100 nm) that will have a higher chance to nucleate and form cloud droplets, as long as they are hygroscopic.

In an attempt to quantify the relation between the aerosol mass and the $T-r_e$ profile, each profile needed to be characterized by one single number. A good candidate was the temperature difference between the cloud-base and the temperature at which the 30th percentile r_e crossed $14 \mu\text{m}$ (henceforth, ΔT_{14}), because this corresponds to the temperature or the height at which the cloud starts to produce precipitation sized particles (Rosenfeld and Guttman, 1994). We visually tested this assumption by comparing precipitation radar images (not shown here) with the satellite images and found that indeed clouds with $r_e < 14 \mu\text{m}$ generally did not have any radar precipitation echoes. ΔT_{14} takes into account the different cloud base temperatures and can be translated to the cloud depth required for the initiation of the precipitation (Δh_{14}) by the pseudo-adiabatic lapse rate. The six profiles that did not reach the precipitation threshold of $14 \mu\text{m}$ had no value for ΔT_{14} and therefore had to be left out (extrapolation of these profiles would have been problematic due to their complex and non linear nature). Figure 8a shows the relation

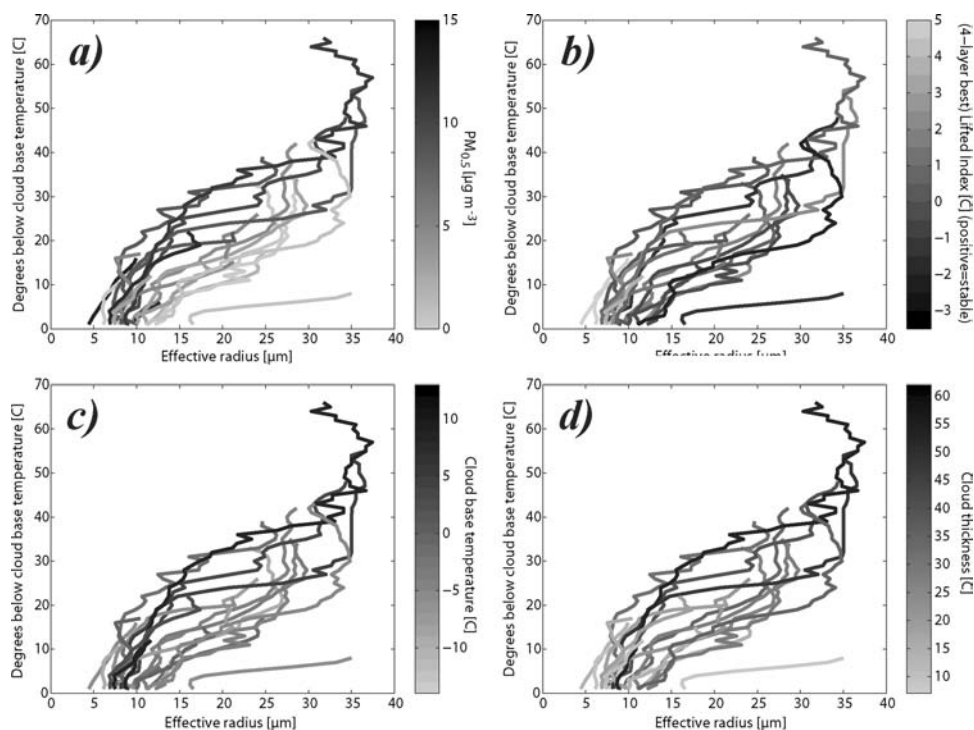


Fig. 7. Same as in Fig. 6 but cloud top temperature is normalized to account for the different cloud base temperatures for all (21) independent profiles (southern Sweden, April–August 2004). Profiles are shaded according to different parameters: (a) $PM_{0.5}$ in Aspövreten or Vavihill (whichever was closer to the cloud domain); (b) the (four-layer best) Lifted Index; (c) the temperature of the cloud base (warmest cloudy pixel in the cloud domain) and (d) the vertical extent of the profile.

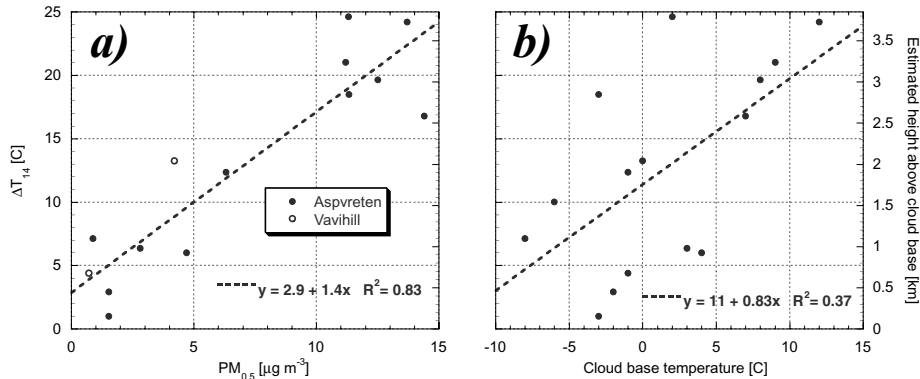


Fig. 8. The relationship between the temperature at which the profile of the 30th percentile r_c crosses $14 \mu\text{m}$ (ΔT_{14} – left vertical axis) and (a) $\text{PM}_{0.5}$ measured at Aspvreten (full circles) or Vavihill (empty circles) (b) the cloud base temperature, for all profiles that cross the precipitation threshold (15 of 21 cases, but no $\text{PM}_{0.5}$ for one of the 15 cases so 14 points are plotted in panel (a)). The right vertical axis shows the estimation of the height above the cloud base for the onset of precipitation (Δh_{14}). The dashed lines show the linear fit. Note the small scattering in panel (a) compared to panel (b) indicating high correlation coefficient.

between $\text{PM}_{0.5}$ and ΔT_{14} for the 14 cases with both measurements, it also displays the estimated cloud depth required for the production of precipitation sized particles (Δh_{14}). The linear correlation coefficient between $\text{PM}_{0.5}$ and ΔT_{14} (or Δh_{14}) is 0.91 (Table 2). This means that in our limited, yet not very small sample, $\text{PM}_{0.5}$ (observed at one of the nearest ground stations) alone can explain more than 80% of the variability in ΔT_{14} (the coefficient of determination R^2 equals 0.83). This number is surprisingly high considering the fact that these profiles were calculated for clouds in different areas, atmospheric stabilities, and range of base temperatures, heights and vertical extents, and because the $\text{PM}_{0.5}$, which was sometimes derived from measurements hundreds of kilometres away from the cloud domain, does not account for the specific aerosol size distribution and chemical composition despite their role in cloud droplet nucleation.

The above-mentioned small apparent structure in the tint of the profiles, grey-shaded according to their cloud base temperatures (Fig. 7c), is translated into a linear correlation coefficient of 0.61 between ΔT_{14} and the cloud base temperature (Fig. 8b and Table 2). This relation can be explained by the fact that clouds with colder bases are expected to reach the ice phase closer to their bases, thus increasing r_c and decreasing ΔT_{14} . But a linear regression model even including cloud base temperature does not improve the explained variability in ΔT_{14} . We suggest that this is because the cloud base temperature and aerosol mass are interrelated to some extent ($R = 0.51$) through the origin of the air-mass, as polar or arctic air-masses are relatively cold and at the same time tend to have smaller aerosol masses than warmer air arriving from the south.

On the other hand, although the cloud thickness or the cloud top temperature (correlation of $R = -0.91$ between them) are less strongly correlated with ΔT_{14} , either of them, together with $\text{PM}_{0.5}$ as independent variables in a linear regression model, improves the explanation of the ΔT_{14} variance (R^2) by an ad-

ditional 6–7% to 89%, compared to the linear model including only $\text{PM}_{0.5}$. These two parameters seem to be related (but not significantly) to the instability parameters (CAPE and LI) but not to $\text{PM}_{0.5}$. In addition, the concept of aerosols suppressing rain and by that causing the intensification of the convection and the elevation of cloud tops (Koren et al., 2005), might be hidden in the relation between ΔT_{14} and cloud thickness (or cloud top temperature). But further investigation of many more cases is needed to separate the effect of the atmospheric instability both on ΔT_{14} and on the cloud thickness.

$\text{PM}_{2.5}$ and PM_{10} were found to be less correlative with ΔT_{14} compared to $\text{PM}_{0.5}$, as expected, because they are very sensitive to the relatively small number of supermicron aerosols.

As previously mentioned, $\text{PM}_{0.5}$ is not directly responsible for the variability in ΔT_{14} . Its strong relation to ΔT_{14} is due to its sensitivity to the number of accumulation mode particles that contribute the most to the activated CCNs, and therefore can substitute CCN concentration measurements. Figure 9 shows the linear correlation coefficient between ΔT_{14} and the number concentration of aerosols larger than various cut-off diameters (in the horizontal axis, henceforth, N_x , where ‘x’ represents the cut-off diameter). N_x does not include particles larger than 500 nm, as it is the largest detectable aerosol diameter by the DMPS at Aspvreten. But its value would not change much, even if we were able to include the number of particles larger than 500 nm as their concentration is usually very small in relation to the smaller particles’ concentration. It is evident in Fig. 9 that ΔT_{14} correlates fairly well with the entire cut-off diameter range that is shown (45–250 nm) and it peaks for N_{140} . This means that on average, the number of aerosols larger than 140 nm can best predict ΔT_{14} , but it does not necessarily mean that smaller particles do not activate, as the chemical composition of the aerosols also have a role in CCN activation. The small peak in the correlation near the diameter of 60 nm requires further investigation in order to

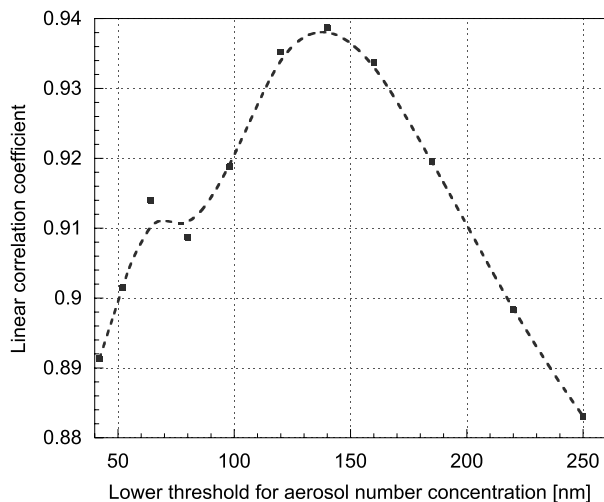


Fig. 9. The linear correlation coefficient between ΔT_{14} and the number concentration of aerosols larger than different thresholds, as marked on the horizontal axis, for the 14 cases out of 20 profiles that exhibited precipitation and had $PM_{0.5}$ measurements. The dashed line is the smoothed curve.

find out whether it has a physical meaning or only an effect due to the limited number of cases investigated.

The strong correlation between $PM_{0.5}$ and ΔT_{14} shown in Fig. 8a and Table 2 is biased by the omission of six profiles that do not reach or cross the $14 \mu\text{m}$ precipitation threshold (see Table 1) because they are too shallow (low dynamic forcing) and/or have an extremely continental behaviour. According to the regression in Fig. 8a and the scattering of the data points, at least two of these cases should have crossed the precipitation threshold, based on the $PM_{0.5}$ and their vertical extent, but they do not. This indicates that in some cases additional information (e.g. specific aerosol size distribution and composition, atmospheric stability) is needed for predicting ΔT_{14} accurately.

4. Summary and conclusions

This study shows that despite the relatively moderate levels of anthropogenic pollution in southern Sweden compared to other places in the world, it is indeed possible to detect significant differences in cloud microphysics between ‘natural’ low- $PM_{0.5}$ and anthropogenic-affected (higher $PM_{0.5}$) air-masses even within rather small changes in the aerosol mass. Similar studies were previously concentrated on lower-latitude areas with stronger thermodynamic driving forces or areas with aerosol loadings typically larger by an order of magnitude compared to the most polluted days in this study.

The anthropogenic aerosols were found to be suppressing the precipitation processes in the convective clouds in a gradual manner, that is, there was a high linear correlation between the aerosol mass (of particles smaller than 500 nm in diameter) in the boundary layer and the cloud depth required for the clouds to produce

precipitation sized particles (Δh_{14}). The aerosol mass was, in turn, related to the origin of the air-mass: low aerosol masses were associated with air-masses arriving from between the north and the west with almost no anthropogenic influence, but occasionally with significant natural contribution to the aerosol number during nucleation events. High aerosol masses, on the other hand, were linked mainly to air-masses that approached Sweden from between the south and the east, after passing above continental Europe and taking up numerous anthropogenic aerosols that could act as CCN and affect the cloud microphysics.

The change in the precipitation patterns caused by the additional anthropogenic aerosols also induces changes in the radiation balance of the atmosphere, as heat is moved to different parts of the atmosphere (the so-called ‘second aerosol indirect effect’). This emphasizes the importance of explicitly including aerosol processes in cloud-radiation models and in climate change studies, not only to account for the well known ‘Twomey effect’, but also for the less documented, more complex and potentially even more important precipitation pattern changes caused by anthropogenic aerosols.

Apparently, the relation between the aerosol mass and cloud microphysics had no significant seasonal dependence (within the period of April to August 2004), maybe except for the relation to the generally rising cloud base temperature within that period. The cloud base temperature was, in turn, found to be the second most correlative factor with ΔT_{14} , just before the vertical extent of the cloud, but including both variables (aerosol mass and cloud base temperature) in a linear regression model, did not improve the explanation of the ΔT_{14} variability. However, including the cloud vertical extent improved the explanation by 6–7%.

The effects of each additional $1 \mu\text{g m}^{-3}$ of aerosols (smaller than 500 nm) to the boundary layer air (equivalent to ~ 150 accumulation mode particles per cc), was estimated to increase Δh_{14} by 220 m ($156\text{--}281 \text{ m}$ is the 95% confidence interval). This means that in high $PM_{0.5}$ occasions, in cases when the thermodynamic conditions of the atmosphere are not allowing the convective clouds to develop to heights where they should precipitate according to the $PM_{0.5}$, the clouds will probably not precipitate during their lifetime. These clouds would probably have precipitated if they were not affected by the anthropogenic pollution that led to the high $PM_{0.5}$ in the first place. Therefore, taking into account aerosol loading in probability based summertime convective precipitation prediction, might be beneficial. But it is important to mention that this strong relation between aerosol mass and cloud microphysical behaviour might not hold in events such as aerosol nucleation, which is usually characterized by very low aerosol mass. In such cases, the small and numerous nucleation mode aerosols, can grow into Aitken mode ($\sim 30\text{--}100 \text{ nm}$) and form a steep distribution from which a significant fraction could be CCN. The result would be clouds with a ‘polluted’ microphysical behaviour despite very low aerosol mass. In order to know how often this is the

case and to understand better the causes of such requires further investigation and probably chemical or CCN measurements in conjunction with model validation and detailed aerosol size measurements.

5. Acknowledgments

This work is in part supported by the Swedish EPA and the Swedish Research Council. Thanks to Adam Kristensson for providing Vavihill data and Daniel Michelson (SMHI) for providing the Radar images. Special thanks to O. Burstein at the Hebrew university of Jerusalem for the assistance with the satellite image analysis.

References

- Andreae, M. O., Rosenfeld, D., Artaxo, P., Costa, A. A., Frank, G. P. and co-authors. 2004. Smoking rain clouds over the Amazon. *Science* **303**, 1337–1342.
- Freud, E., Rosenfeld, D., Andreae, M. O., Costa, A. A. and Artaxo, P. 2005. Robust relations between CCN and the vertical evolution of cloud drop size distribution in deep convective clouds. *Atmos. Chem. Phys. Discuss.* **5**, 10155–10195.
- Heymsfield, A. J. and McFarquhar, G. M. 2001. Microphysics of IN-DOEX clean and polluted trade cumulus clouds. *J. Geophys. Res.* **106**(D22), 28653–28673, doi:10.1029/2000JD900776.
- Hudson, J. G., Hallett, J. and Rogers, C. F. 1991. Field and laboratory measurements of cloud forming properties of combustion aerosols. *J. Geophys. Res.* **96**(D6), 10847–10859.
- Hudson, J. G. and Yum, S. S. 2001. Maritime-continental drizzle contrasts in small cumuli. *J. Atmos. Sci.* **58**, 915–926.
- Kaufman, Y. L. and Fraser, R. S. 1997. The effect of smoke particles on clouds and climate forcing. *Science* **277**, 1636–1639.
- Kavouras, I. G., Mihalopoulos, N. and Stephanou, E. G. 1998. Formation of atmospheric particles from organic acids produced by forests. *Nature* **395**, 683–686.
- Khain, A., Pokrovsky, A., Pinsky, M., Seifert, A. and Phillips, V. 2004. Simulation of effects of atmospheric aerosols on deep turbulent convective clouds using a spectral microphysics mixed-phase cumulus cloud model. Part I: model description and possible applications. *J. Atmos. Sci.* **61**(24), 2963–2982.
- Koren, I., Kaufman, Y. J., Rosenfeld, D., Remer, L. A. and Rudich, Y. 2005. Aerosol invigoration and restructuring of Atlantic convective clouds. *Geophys. Res. Lett.* **32**, L14828, doi:10.1029/2005GL023187.
- Kulmala, M., Vehkamäki, H., Petäjä, T., Dal Maso, M., Lauri, A. and co-authors 2004. Formation and growth rates of ultrafine atmospheric particles: a review of observations. *Aer. Sci.* **35**, 143–176.
- Lensky, I. M. and Rosenfeld, D. 2005. The time-space exchangeability of satellite retrieved relations between cloud top temperature and particle effective radius. *Atmos. Chem. Phys. Discuss.* **5**, 11911–11928.
- Nober, F., Graf, H. F. and Rosenfeld, D. 2003. Sensitivity of the global circulation to the suppression of precipitation by anthropogenic aerosols. *Global Plan. Chan.* **37**, 57–80.
- O'Dowd, C. D., Aalto, P., Hämeri, K., Kulmala, M. and Hoffmann, T. 2002. Atmospheric particles from organic vapors. *Nature* **416**, 497–498.
- Parikh, J. 2000. PM_{2.5} Tapered Element Oscillating Microbalance Procedure. State of Washington – Department of Ecology – Air Quality Program, 42 pp.
- Patashnick, H. and Rupprecht, E. G. 1991. Continuous PM-10 measurement using the tapered element oscillating microbalance. *J. Air Waste Manag. Assoc.* **41**, 1079–1083.
- Rosenfeld, D. 1999. TRMM Observed First Direct Evidence of Smoke from Forest Fires Inhibiting Rainfall. *Geophys. Res. Lett.* **26**(20), 3105–3108.
- Rosenfeld, D. 2000. Suppression of Rain and Snow by Urban and Industrial Air Pollution. *Science* **287**, 1793–1796.
- Rosenfeld, D. and Gutman, G. 1994. Retrieving microphysical properties near the tops of potential rain clouds by multispectral analysis of AVHRR data. *Atmos. Res.* **34**, 259–283.
- Rosenfeld, D. and Lensky, M. I. 1998. Satellite Based Insights into Precipitation Formation Processes in Continental and Maritime Convective Clouds. *Bull. Amer. Meteor. Soc.* **79**(11), 2457–2476.
- Rosenfeld, D., Rudich, Y. and Lahav, R. 2001. Desert dust suppressing precipitation—a possible desertification feedback loop. *Proc. Natl Acad. Sci.* **98**, 5975–5980.
- Rosenfeld, D., Lahav, R., Khain, A. and Pinsky, M. 2002. The role of sea spray in cleansing air pollution over ocean via cloud processes. *Science* **297**, 1667–1670.
- Schwab, J. J., Felton, H. D., Rattigan, O. V. and Demerjian, K. L. 2006. New York State Urban and Rural Measurements of Continuous PM_{2.5} Mass by FDMS TEOM and BAM: Evaluations and comparisons with the FRM. *JAWMA* **56**, 372–383.
- Tunved, P., Hansson, H. C., Kulmala, M., Aalto, P., Viisanen, Y. and co-authors 2003. One year boundary layer aerosol size distribution data from five Nordic background stations. *Atmos. Chem. Phys.* **3**, 2183–2205.
- Tunved, P., Nilsson, E. D., Hansson, H. C., Kulmala, M., Aalto, P., and co-authors. 2005. Aerosol characteristics of air masses in Northern Europe—influences of location, transport, sinks and sources. *J. Geophys. Res.* **110**, D07201, doi:10.1029/2004JD005085.
- Tunved, P., Hansson, H.-C., Kerminen, V.-M., Ström, J., Lihavainen, H. and co-authors. 2006. High natural aerosol loading over boreal forests. *Science* **312**, 261–263, doi:10.1126/science.1123052.
- Twomey, S. 1974. Pollution and the planetary albedo. *Atmos. Environ.* **8**, 1251–1256.
- Yum, S. S. and Hudson, J. G. 2002. Maritime/continental microphysical contrasts in stratus. *Tellus* **54B**, 61–73.